BIS ENERGY AND ENGINEERING

Volume 4 2026 | DOI: 10.31603/biseeng.560
7th Borobudur International Symposium on Science and Technology (BIS-STE) 2025

UNIMMA PRESS
Universitas Muhammadiyah Magelang

Hydraulic and numerical analysis of non-uniform and two-phase wastewater flow in sewer pipelines

Shakhzodbek Umurkulov[1], Jahongir Orzimatov[1*], Ismoil Nasirov[1], Durdona Davronova[1], and Islomjon Inomjonov[1]

[1] Faculty of Architecture and Construction, Fergana State Technical University 86, Fergana, Uzbekistan
[*] Corresponding author's email: jaxongirorzimatovfarpi@gmail.com

Abstract

This article examines the characteristics of non-uniform and two-phase (water–air) wastewater flow in sewer systems. Non-uniform flow, caused by sediment formation and operational condition changes, can lead to sludge buildup and decreased system efficiency. Classical equations of non-uniform flow, including critical depth and drawdown length calculations, are applied for hydraulic analysis. In the numerical part, the ANSYS software suite is used to simulate two-phase flow with VOF (Volume of Fluid) and DPM (Discrete Phase Model), as well as the GEKO turbulence model. The results enable visualization of spatial water and air distribution within pipes, evaluate particle behavior of various densities, and determine how pipeline slopes influence flow patterns. The analysis emphasizes the necessity of considering both non-uniform and two-phase flow regimes in the design and operation of sewer systems.

Keywords

Non-uniform flow, Wastewater, Sewer system, Pipeline slope, Pumerical modeling, Velocity

Introduction

Hydraulic processes in sewer systems play a crucial role in ensuring reliable and efficient transportation of wastewater from the user to treatment facilities. Most sewer system designs are based on calculations assuming uniform and steady flow. However, real-world operation often involves variable flow regimes due to design characteristics and operational conditions, such as fluctuating loads, irregular wastewater inflow, and external interferences. Non-uniform flow is especially common in areas with changing slopes, near junctions and drop manholes, and at terminal sections leading to pump stations. In these zones, backwater or drawdown areas may form, causing significant changes in hydraulic conditions. These effects not only complicate system operation but also create conditions for pipe silting, reduced flow velocity, and stagnant zones [1], [2],[3], [4], [5].

Published:
May 04, 2026

Selection and Peer-review under the responsibility of the 7th BIS-STE 2025 Committee

Classical hydraulic equations, such as Bernoulli's energy equation and the Sen-Benana equation, can quantitatively describe flow behavior in individual sections of the system. A particularly important parameter in analysis is the critical depth-the boundary between tranquil and rapid flow regimes-which plays a key role in designing sections with varying cross-sections and slopes. Calculations have shown that neglecting these factors can lead to inaccurate assessments of pipe capacity and systemic failures during peak loads. Therefore, modern engineering calculations should include non-uniform flow evaluations, refined hydraulic models, and flow behavior predictions along pipeline length. This is especially crucial amid increasing urbanization and pressure on sewer systems [6], [7].

In addition to analytical methods, numerical modeling techniques have gained significant traction in recent decades for studying complex flows in engineering systems. One such powerful tool is ANSYS Fluent, which enables simulation of multiphase flows, including two-phase media and discrete particle movement [8], [9], [10].

This study focuses particularly on modeling interactions between liquid (water) and gas (air) phases with solid inclusions particles of varying densities. Two key models are used: VOF (Volume of Fluid) for tracking phase interfaces, and DPM (Discrete Phase Model) for analyzing particle motion and deposition. Turbulent flow is described using the GEKO model, allowing for consideration of vortex influence and local velocity variations on particle transport [11], [12], [13], [14], [15]. Numerical experiments are conducted for pipes with different slopes (i = 0.008 and i = 0.01), establishing a clear correlation between pipe geometry and particle sedimentation intensity. As slope increases, flow velocity rises, phase distribution becomes more uniform, and sediment concentration decreases. Conversely, with a shallow slope, flow energy is lost, particle motion slows, and sedimentation intensifies especially at the pipe's lower cross-section.

The obtained numerical data have been visualized in the form of velocity isolines, concentration fields, and graphs of phase volume fractions at various distances from the inlet (L = 12.5D, 25D, 37.5D). These results not only confirm previously obtained analytical estimates but also clearly demonstrate the processes occurring within the system, including potential sedimentation risk zones and the conditions under which they form. Thus, numerical modeling serves as an effective tool for verifying and complementing classical hydraulic approaches and can be used to optimize design decisions in modern wastewater systems.

The scientific novelty of this work lies in the comprehensive approach to analyzing non-uniform and two-phase wastewater flow in sewer pipelines, combining classical hydraulic calculations with modern numerical modeling in the ANSYS software environment. For the first time, it is shown how changes in pipeline slope affect the intensity of particle sedimentation of varying densities in a two-phase flow. Additionally, the ability to accurately localize potential sedimentation zones using the VOF and DPM

models is demonstrated, which significantly improves the efficiency of designing and operating sewer systems under variable hydraulic conditions.

Hydraulic analysis of non-uniform wastewater flow

The differential equation for steady, gradually varied flow in a circular pipe can be written as.

$$\frac{i_\theta dl}{D} = \frac{K^2/K_p^2\left[1-\alpha Q^2 B/\left(g\omega^3\right)\right]}{\frac{K^2}{K_p^2}-Q^2/Q_p^2}, \quad (1)$$

Where $K_п$ и $Q_п$ – are the discharge module and water discharge in a fully filled collector.

Expressing $K^2/K_p^2 = C\alpha^{\beta}$ (where for $0{,}15 \le \alpha \le 0{,}5$ C=3,73 and $\beta = 3{,}9$ for $0{,}5 \le \alpha \le 0{,}9$ C=1.23 and $\beta = 2.3$) and $\frac{\omega^3}{BD^5} = \alpha^{3.9}/1.093$

we get

For case a ≤ 0.5

$$\frac{i_\theta l}{D} = \alpha_2 - \alpha_1 + \left(1 - \frac{4.07\alpha Q_p^2}{gD^5}\right)x \left[\frac{\alpha_1}{\left(1-3.73\alpha_1^{3.9}Q_п^2/Q^2\right)^{0.204}} - \frac{\alpha_2}{\left(1-3.73\alpha_1^{3.9}p/Q^2\right)^{0.204}}\right], \quad (2)$$

For case $\alpha \ge 0.5$

$$\frac{i_\theta l}{D} = \alpha_2 - \alpha_1 + \left(1 - \frac{1.34\alpha Q_p^2}{gD^5\alpha_{sr}^{1.6}}\right)x \left[\frac{\alpha_1}{\left(1-1.23\alpha_1^{2.8}Q_p^2/Q^2\right)^{0.303}} - \frac{\alpha_2}{\left(1-1.23\alpha_2^{2.8}Q_п^2/Q^2\right)^{0.303}}\right], \quad (3)$$

For a horizontally laid collector (i=0)

For case $\alpha \le 0.5$

$$\frac{l}{D} = 0.762\frac{K_п^2}{Q^2}\left[\frac{5.35\alpha Q^2}{gD^5}(\alpha_2 - \alpha_1) - \alpha_2^{4.9} + \alpha_1^{4.9}\right], \quad (4)$$

For case $\alpha \le 0.5$

$$\frac{l}{D} = 0.375\frac{K_п^2}{Q^2}\left[\frac{6\alpha Q^2}{gD^5}\left(\frac{1}{\alpha_1^{0.6}} - \frac{1}{\alpha_2^{0.6}}\right) - \alpha_2^{3.3} + \alpha_1^{3.3}\right], \quad (5)$$

When the free surface curve passes through the pipe's midpoint, calculations must first proceed from the initial section $\alpha_1 = \alpha_н$ up to the section with half pipe filling $\alpha_2 = 0.5$ pipe filling, and then from the filling a=0,5 to the final section using the corresponding formulas (2) – (5).

The critical depth at the end of the drawdown curve before the drop can be determined by the formula.

$$\alpha_{cr} = \frac{h_{kp}}{D} = 1.023\left(\sqrt{\alpha/g}Q/D^{5/2}\right)^{0.511}, \quad (6)$$

The values of pipeline length and flow rate for free surface flow from full filling at the beginning $\alpha_н = 1$ to critical depth $\alpha_{кр}$ at the end are derived from the following Table 1.

Table 1. Horizontal pipeline

α_{cr},	0.95	0.9	0.8	0.7	0.6	0.5	0.4	0.3
$\sqrt{\alpha/g}Q/D^{5/2}$	1.02	0.835	0.62	0.47	0.35	0.246	0.163	0.096
$\frac{Q^2}{K_p^2}$l/D	0.017	0.035	0.082	0.197	0.197	0.254	0.298	0.329
$\lambda_p l/\alpha D$	0.02	0.062	0.264	0.755	1.99	5.18	13.9	44.2

With free surface outflow from a horizontal pipeline, the pipe is never fully filled at the end—even under high discharges and over short distances.

Under free-surface non-uniform outflow with a drop at the end, the pipeline can carry greater discharges than in uniform flow. The pipeline parameters $\frac{i_\theta l}{D}$ и $\lambda_p l/\alpha D$ under which the filling of the pipe (laid at a slope of i_θ) decreases from full at the beginning ($\alpha_н = 1$) to critical $\alpha_{кр}$, at the end, under flow rates exceeding those for full pipe filling (Q/Q_p>1) can be found using Figure 1.

Results and discussion

Hydraulic analysis

Example 1. Find the flow depth at the end of a pipeline with diameter D=1 м, length l =683 м, and slope i_θ=0,0006 when discharging Q=723 l/s

"Based on the given input data, we obtain $Q_п$=603 l/s, Q/Q_p=723/603=1,2 From the graph (Figure 1) as $\frac{i_\theta l}{D}$=0,0006·683/1=0,41 and Q/Q_p=1,2 find α_k=0,5 At this flow rate, we obtain $\sqrt{\alpha/g}Q/D^{5/2}$=$\sqrt{1{,}1/9{,}81}\cdot\frac{0{,}723}{1}=0{,}244$, what corresponds to the relative critical depth α_k=0,5. Thus, over the specified length of the pipeline, the degree of pipe filling will decrease from full to critical. If the length of the pipeline is shorter than the specified one, then its filling will be incomplete.

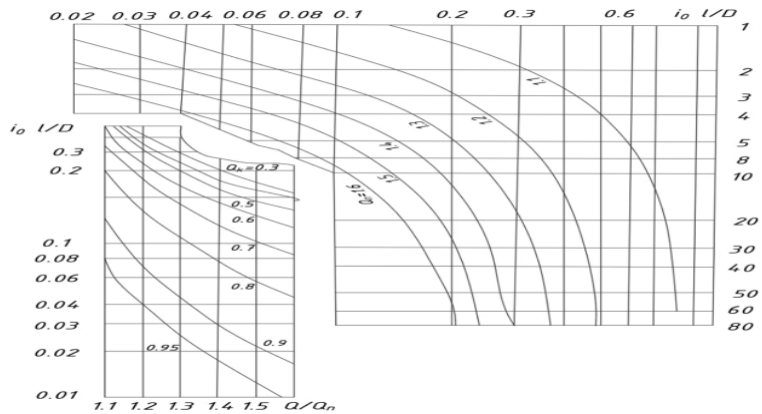

Figure 1. Dependence $i_0\frac{l}{D}$от $\lambda_п = (2\alpha i_0)$ and from $Q/Q_п(b)$ For non-uniform flow of water in a pipe with a decreasing (falling) profile

Example 2 At the end of the collector with diameter D=1500 мм, laid with a slope i_θ =0,001 and at a filling ratio h/D=0,75 carrying a flow rate Q =1834 l/s, there is a pumping

station with a receiving reservoir. The invert elevation of the collector at the receiving reservoir of the pumping station is +15 m. Determine the elevation of the wastewater level in the receiving reservoir during uniform flow in the collector, as well as the possible minimum elevation of the flow level at the outlet section of the collector.

The depth of uniform flow in the collector is found from the given filling ratio $h_0 = 75\ D = 0.75\ \cdot 1500 = 1.125$ м.

At this depth, the wastewater level elevation in the receiving reservoir of the pumping station is 15+$h_0 = 15 + 1{,}125 = 16{,}125$ м

If the water level in the receiving reservoir of the pumping station rises above 16.125 m, backwater will begin to form in the collector, which may cause sedimentation due to reduced velocity.

Next, calculate the critical depth using formula (6)

$$h_{cr} = 1{,}023(\sqrt{1{,}1/9{,}81} \cdot 1{,}834/1{,}5^{5/2})^{0{,}511} \cdot 1{,}5 = 0{,}71 \text{ м}$$

Minimum wastewater level elevation at the end of the collector

$$15 + h_{cr} = 15 + 0{,}71 = 15{,}71 \text{ м}$$

This level will remain unchanged for any water level in the receiving reservoir below 15.71 m. It is known that when $h_0 > h_{кр}$ the flow condition is tranquil, and when $h_0 < h_{cr}$ – it is rapid (turbulent). In this case, $h_0 = 1{,}125$ м $> h_{cr} = 0.71$ м, meaning the flow condition in the collector is tranquil.

Numerical simulation of particle settling in ANSYS depending on the pipeline slope

1. Mathematical and physical formulation of the problem

The geometric model of the inclined pipeline is shown in Fig. 2, created in ANSYS. The blue color indicates the inlet section (Inlet), through which a two-phase flow (water and air) is supplied. The red color indicates the outlet section (Outlet), where free liquid outflow occurs. The internal view of the computational domain with an overlaid three-dimensional mesh is shown. A well-detailed mesh in the pipe's cross-section is visible, ensuring the accuracy of numerical modeling of turbulent and interphase interactions.

The initial distribution of phases (water and air) is homogeneous. The pressure in the computational domain corresponds to atmospheric pressure (101,325 Pa). The initial velocity in the pipeline is assumed to be uniform and directed along the pipe axis.

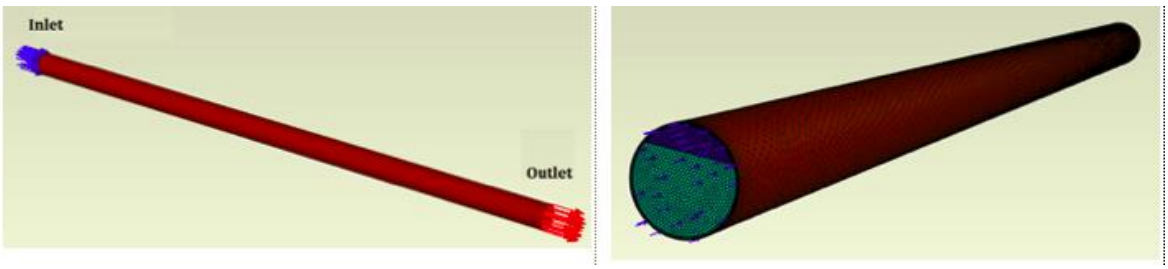

Figure 2. Principal scheme and computational mesh Initial and boundary conditions of the problem

a. Boundary conditions

Inlet Type: velocity inlet Flow velocity is given as a vector, for example U_{in}=1 м/. volume fraction of water: 0.9 (90%), volume fraction of air: 0.1 (10%), Outlet: Type: pressure outlet. Pressure: atmospheric (0 Pa gauge pressure), Pipe walls (Wall): Type: no-slip boundary condition. All velocity components are zero at the walls, no interphase slip occur.

For the numerical study of the posed problem, the Reynolds-averaged Navier–Stokes (RANS) equations [16] are used. These equations consider the effect of turbulence by adding turbulent stresses that arise from averaging the unsteady flow. In general form, the motion equation for an incompressible fluid considering turbulence is written as follows.

$$\begin{cases} \dfrac{\partial \rho}{\partial t}+\dfrac{\partial\left(\bar{U}_i\right)}{\partial x_j}=0, \\ \dfrac{\partial\left(\rho \bar{U}_i\right)}{\partial t}+\dfrac{\partial\left(\rho \bar{U}_i \bar{U}_j\right)}{\partial x_j}=-\dfrac{\partial p}{\partial x_i}+\rho \bar{G}+\dfrac{\partial}{\partial x_j}\left[(\mu+\mu_t)\left(\dfrac{\partial \bar{U}_i}{\partial x_j}+\dfrac{\partial \bar{U}_j}{\partial x_i}\right)\right]. \end{cases} \tag{7}$$

The GEKO (Generalized k-ω) turbulence model [13], [14], developed by Ansys, is an extension of the standard SST (Shear Stress Transport) model and is designed to improve the flexibility and accuracy of turbulent flow simulations. Due to its versatility, GEKO is an effective tool for modeling complex hydraulic processes.

$$\begin{cases} \dfrac{\partial(\rho k)}{\partial t}+\dfrac{\partial\left(\rho \bar{U}_j k\right)}{\partial x_j}=P_k-C_\mu \rho k \omega+\dfrac{\partial}{\partial x_j}\left[\left(\mu+\dfrac{\mu_t}{\sigma_k}\right)\dfrac{\partial k}{\partial x_j}\right], \\ \dfrac{\partial(\rho \omega)}{\partial t}+\dfrac{\partial\left(\rho \bar{U}_j \omega\right)}{\partial x_j}=C_{\omega 1} F_1 \dfrac{\omega}{k} P_k-C_{\omega 2} F_2 \rho \omega^2+\rho F_3 CD+\dfrac{\partial}{\partial x_j}\left[\left(\mu+\dfrac{\mu_t}{\sigma_\omega}\right)\dfrac{\partial \omega}{\partial x_j}\right]. \end{cases} \tag{8}$$

Turbulent eddy viscosity is calculated using: $\mu_t=\rho \nu_t=\rho \dfrac{k}{\max\left(\omega, S / C_{Realize}\right)}$.

$$P_k=-\tau_{ij} \frac{\partial U_i}{\partial x_j}, \tag{9}$$

$$\tau_{ij}^{EV}=-\rho \overline{u_i' u_j'}=\mu_t 2 S_{ij}-\frac{2}{3} \rho k \delta_{ij}, \tag{10}$$

$$CD = \frac{2}{\sigma_\omega}\frac{1}{\omega}\frac{\partial k}{\partial x_j}\frac{\partial \omega}{\partial x_j}, \tag{11}$$

$$\tau_{ij} = \tau_{ij}^{EV} - C_{CORNER}\frac{1.2\mu_t}{\max\left(0.3\omega, \sqrt{0.5\left(S^2+\Omega^2\right)}\right)}\left(S_{ik}\Omega_{kj} - \Omega_{ik}S_{kj}\right), \tag{12}$$

$$S_{ij} = \frac{1}{2}\left(\frac{\partial U_i}{\partial x_j} + \frac{\partial U_j}{\partial x_i}\right),\ \Omega_{ij} = \frac{1}{2}\left(\frac{\partial U_i}{\partial x_j} - \frac{\partial U_j}{\partial x_i}\right),$$
$$S = \sqrt{2S_{ij}S_{ij}},\ \Omega = \sqrt{2\Omega_{ij}\Omega_{ij}}. \tag{13}$$

The remaining coefficients and functions were presented in the article. [16].

b. Multiphase model

To track the free surface between the liquid (water) and gas (air) phases, the Volume of Fluid (VOF) method is used. VOF is a Eulerian-type method in which the volume fraction occupied by each phase is tracked in every computational cell. In this study, the VOF (Volume of Fluid) multiphase model was used to simulate this phenomenon. It demonstrated high accuracy in predicting the shape and evolution of the air core, as confirmed in previous studies [18]. The VOF model is based on a fully Eulerian approach and is designed to track the interface between two continuous phases. In the considered hydrocyclone, the boundary between air and water is modeled using the transport equation (14).

$$\frac{\partial a_p}{\partial t} + a_p\frac{\partial u_i}{\partial x_i} = 0, \tag{14}$$

where α_p represents the volume fraction of the n-th phase. The average density is described as follows:

$$\rho = a_p\rho_{water} + \left(1+a_p\right)\rho_{air}. \tag{15}$$

RANS–VOF modeling is achieved through Favre averaging, as shown in the work of Fan et al. [19], where the formulation for equation (8) is derived in terms of the volume-averaged volume fraction.

c. Particle Tracking

To analyze the operation of the hydrocyclone, it is necessary to consider several key equations. The first describes the motion of particles, and the second — their interaction with the liquid phase. According to [18], the main forces acting on particles in a hydrocyclone are drag force, pressure gradient, and Saffman lift force. Accordingly, the equation of particle motion can be written in the form of the following equation (16).

$$\frac{du_p}{dt} = \left(1 - \frac{\rho_f}{\rho_p}\right) g + F_D\left(u - u_p\right) + \frac{\nabla P}{\rho} + F_s. \quad (16)$$

$F_D\left(u - u_p\right)$— This is the drag force per unit mass. This force is balanced by the centrifugal force. Smooth particles are modeled as small spheres; therefore, the drag term F_D can be written as:

$$F_D = \frac{18\mu}{\rho_p d_p^2} \frac{C_D \mathrm{R_e}}{24}, \quad (17)$$

where the Reynolds number is equal to:

$$\mathrm{R_e} = \frac{\rho_f d_p \left|u_p - u\right|}{\mu}. \quad (18)$$

2. Solution Method

For the numerical simulation of unsteady two-phase flow over a broad-crested weir in ANSYS Fluent, the Volume of Fluid (VOF) model was used in combination with the GEKO turbulence model. The SIMPLE scheme was applied to couple pressure and velocity, ensuring the stability of the calculation. Spatial discretization was performed using second-order schemes: gradients were calculated using the (Least Squares Cell-Based), the PRESTO! scheme was used for pressure; Second Order Upwind was applied for momentum, turbulent kinetic energy, and dissipation rate. The volume fraction was treated using the Compressive scheme, which enabled accurate tracking of the phase interface. Temporal discretization was set to First Order Implicit, providing numerical stability during the simulation of transient processes. To accelerate convergence, the following under-relaxation factors were applied: Pressure — 0.3, Momentum — 0.7, Volume fraction — 0.5, Turbulent kinetic energy and dissipation rate — 0.8, Density, viscosity, and body forces — 1.0. The choice of these parameters ensured a stable and accurate solution in the presence of a free surface and a complex flow structure [14], [15], [16], [17], [18], [19], [20].

3. Calculation results and their discussion numerical modeling

Figure 3 shows the isolines of the results of numerical modeling of a two-phase flow in an inclined pipe.

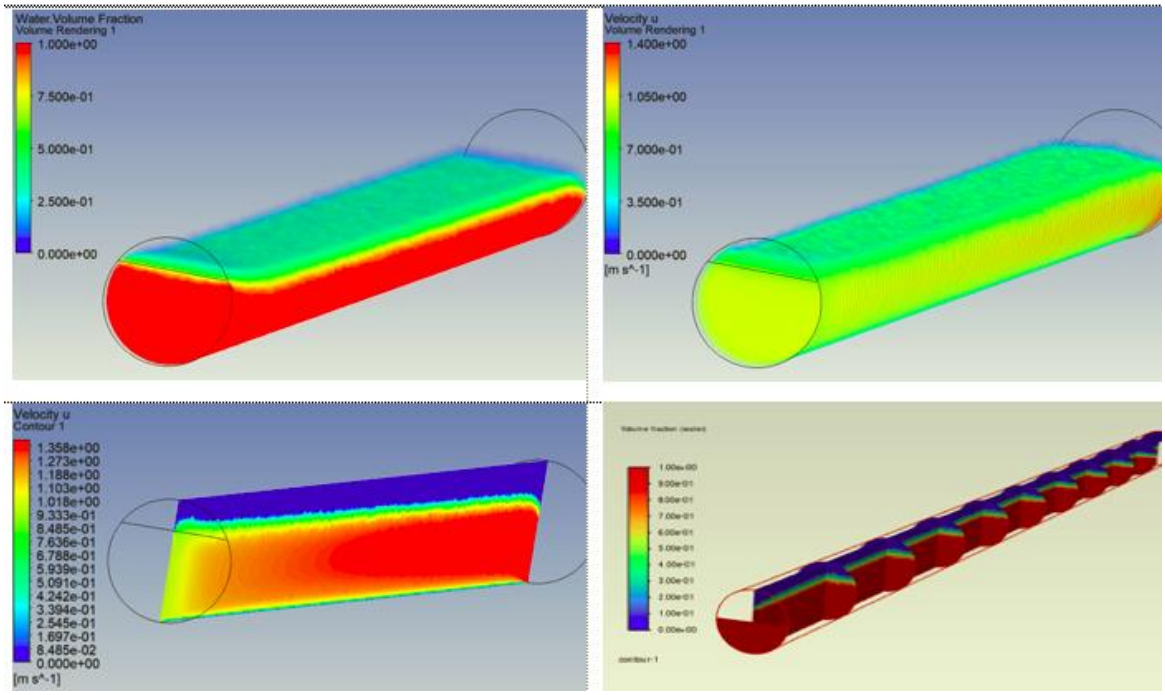

Figure 3. Isolines of the numerical simulation results of two-phase flow in an inclined pipe

Top left plot (Water Volume Fraction): Shows the distribution of the water volume fraction along the length and cross-section of the pipeline. Red areas correspond to full water saturation (volume fraction = 1.0), while blue areas indicate regions occupied by air (volume fraction ≈ 0). As the flow progresses, the water volume fraction gradually decreases near the upper part of the pipe, indicating the influence of inclination and gravity on phase separation. Top right plot (Velocity u – Volume Rendering): Visualization of the volumetric distribution of the longitudinal velocity component (u) along the pipe. The color scale indicates the flow velocity from 0 up to approximately 1.05 m/s. A velocity gradient characteristic of laminar or transitional flow is observed, with maximum velocity closer to the center of the flow. Bottom left plot (Velocity u – Contour): Contour map of the longitudinal velocity component u in the pipe's cross-section. Red zones show areas with the highest velocity, and blue zones indicate areas with minimum or zero velocity near the walls (due to the no-slip condition). This structure confirms the presence of a parabolic velocity profile typical for internal flow. Bottom right plot (Volume Fraction – Section View): Cross-sectional visualization of the water volume fraction along the pipe axis. The results demonstrate the dynamics of two-phase interaction: alternating zones dominated by water and air indicate oscillations or wave-like structures at the phase interface caused by the pipe inclination and hydraulic flow parameters.

Figure 4 presents the results of numerical simulation of particle movement with different densities (ρ = 700–1100 kg/m³) in an inclined pipe at two inclinations: i = 0.008 (left) and i = 0.01 (right). Blue lines indicate the trajectories of particles in the two-phase flow (water + air), visualized based on data from the DPM (Discrete Phase Model).

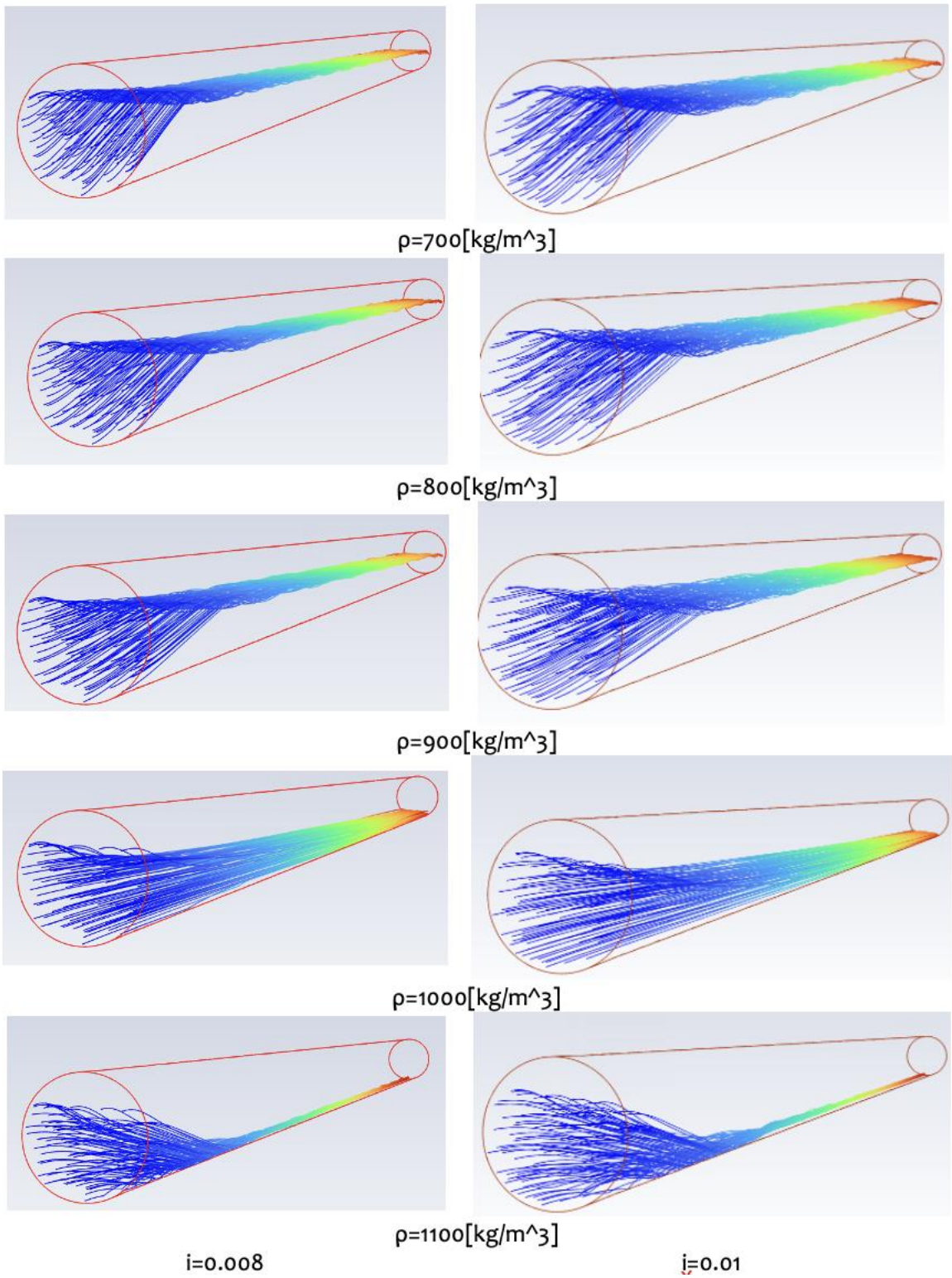

Figure 4. The movement of particles of different densities in an inclined pipe at various inclinations

Main observations:

ρ = 700–800 kg/m³: Low-density particles predominantly move closer to the central and upper parts of the flow. At both inclinations, particles are carried along faster by the main flow, with minimal settling.

ρ = 900 kg/m³: Transitional behavior is observed — particles begin to move closer to the lower part of the pipe but do not settle intensively yet. Inclination i = 0.01 promotes a more uniform distribution across the cross-section.

ρ = 1000 kg/m³: Density approaching that of water increases interaction with the main liquid phase. Particles tend to follow the general flow direction, with a noticeable tendency to settle in the lower zone.

ρ = 1100 kg/m³: High-density particles actively settle at the bottom of the pipe. This behavior is especially pronounced at the lower inclination (i = 0.008), where particle clusters and weak flow carry-over are observed.

Conclusions

The conducted study allowed for a comprehensive analysis of the characteristics of non-uniform and two-phase wastewater flow in inclined pipelines of sewer systems. In the first part of the work, based on classical hydraulic equations, it was shown that non-uniform flow, resulting from pressure drops and changes in geometry, can lead to the formation of stagnation zones, reduced flow velocity, and consequently, sedimentation within the pipes. It was confirmed that accounting for critical depth and the shape of the backwater curve in calculations allows for more accurate determination of conditions for stable network operation. In the second part, using numerical modeling in the ANSYS environment, the behavior of a two-phase flow (water–air) was studied, considering the movement of solid particles of different densities. The use of VOF and DPM models made it possible to visualize phase distribution and evaluate the impact of pipe inclination on particle trajectories and sedimentation. The results showed that at low inclinations and high particle densities, the risk of particle settling and accumulation at the bottom of the pipes significantly increases, which may lead to partial blockages and reduced flow capacity. When the inclination is increased, the flow becomes more energetic, and the particles are more evenly distributed throughout the volume, which promotes self-cleaning of the pipeline.

Thus, the obtained data highlight the necessity of integrating traditional hydraulic calculations with modern numerical modeling methods when designing and optimizing sewer systems. Such a comprehensive approach ensures higher reliability, efficiency, and resilience of network performance under variable flow conditions and complex operational environments.

References

[1] Abdullaev B. et al. Factors affecting the hydrodynamic state of the Sokh groundwater deposit //AIP Conference Proceedings. – AIP Publishing LLC, 2025. – Т. 3256. – №. 1. –С. 040024. https://doi.org/10.1063/5.0267042.

[2] Abdullaev, B., Artikbekova, F., Meliyev, B., Sultonov, A., Suvonova, L., & Alikarieva, D (2025, July). Factors affecting the hydrodynamic state of the Sokh groundwater deposit. In AIP Conference Proceedings (Vol. 3256, No. 1, p. 040024). AIP Publishing LLC.https://doi.org/10.1063/5.0267042.

[3] Glovatskii O. et al. Experience in using methods for monitoring the energy efficiency of hydraulic

systems //IOP Conference Series: Earth and Environmental Science. – IOP. Publishing, 2023. – Т. 1142. – №. 1. – С. 012004. DOI 10.1088/1755-1315/1142/1/012004.
[4] Akhundov, R., Tangirov, A., & Sultonov, A. (2025). Political Dimensions of Global Ecological Governance Frameworks. In BIO Web of Conferences (Vol. 151, p. 02008). EDP Sciences. https://doi.org/10.1051/bioconf/202515102008.
[5] Yu Qian, Weiyun Shao, Khaled.A.A. Modeling air flow in sanitary sewer systems. Journal of Hydro-environment Research Volume 38, September 2021, Pages 84-95. https://doi.org/10.1016/j.jher.2020.10.003
[6] Мельник Ольга Валериевна. Повышение эффективности проектирования и эксплуатации самотечных водоотводящих сетей на базе математического моделирования режима их работы. 2.1.4 - Водоснабжение, канализация, строительные системы охраны водных ресурсов. Москва – 2024.
[7] Дежина Ирина Сергеевна. Повышение транспортирующей способности самотечных трубопроводов с учетом гидрофобности и рельефа их поверхности. 2.1.4. Водоснабжение, канализация, строительные системы охраны водных ресурсов. Москва 2021.
[8] Н.Ф.Федров, А.М.Курганов, М.И.Алексеев. Канализационные сети примеры расчета. Москва, Стройиздат (2016).
[9] Crowe, C. T., Schwarzkopf, J. D., Sommerfeld, M., & Tsuji, Y. (2015). Multiphase flows with droplets and particles. CRC Press
[10] Hu, C., & Liu, C. (2018). Simulation of violent free surface flow by AMR method.Journal of Hydrodynamics, 30, 384–389. https://doi.org/10.1007/s42241-018-0043-4.
[11] Main reserves for increasing the efficiency of solar thermal energy in heat supply systems. Yu K Rashidov, K Yu Rashidov, II Mukhin, Kh T Suratov, JT Orzimatov, Sh Sh Karshiev.
[12] Transition processes during the start-up of the pumping unit of happ. Z.E. Abdulkhaev, M.M. Madraximov, JT Orzimatov, AM Abdurazaqov.
[13] The method of hydraulic calculation of a heat exchange panel of a solar water-heating collector of a tube–tube type with a given nonuniform distribution of fluid flow along lifting pipes. Yu K Rashidov, JT Orzimatov, K Yu Rashidov, ZX Fayziev. Applied Solar Energy 56, 30-34
[14] Подготовка питьевой воды из маломощных поверхностных водоисточников. Зулхумор Кахрамон кизи Ибрагимова, Нозимахон Сохибжон кизи Хамдамова, Шахзодбек Хамдамжон угли Умуркулов, Дониёржон Расулжон угли Сабиров. Central Asian Research Journal for Interdisciplinary Studies (CARJIS), Special Issue 4, 77- 83(2021).
[15] Malikov, Z. M., Mirzoev, A. A., & Madaliev, M. (2022). Numerical simulation of the mixing layer problem based on a new two-fluid turbulence model. Journal of Computational Applied Mechanics, 53(2), 282-296.
[16] Malikov, Z. M., Madaliev, M. E., Navruzov, D. P., & Adilov, K. (2022, October). Numerical study of an axisymmetric jet based on a new two-fluid turbulence model. In AIP Conference Proceedings (Vol. 2637, No. 1). AIP Publishing.
[17] Madaliev, M., Yunusaliev, E., Usmanov, A., Usmonova, N., & Muxammadyoqubov, K. (2023). Numerical study of flow around flat plate using higher-order accuracy scheme. In E3S Web of Conferences (Vol. 365, p. 01011). EDP Sciences.
[18] Madaliev, E., Madaliev, M., Raxmankulov, S., & Raxmonkulova, S. (2023). Turbulent mixing of two plane flows based on the SST turbulence model. In E3S Web of Conferences (Vol. 452, p. 02012). EDP Sciences.
[19] Совершенствование биореакторов для очистки сточных вод. Рахмоналиев Санжар Мухаммаджон ўғли Умуркулов Шахзодбек Хамдамжон ўғли, Сабиров Дониёр Расулжон ўғли. (2021). Models and methods in modern science (volume 2, pages 88), FRENCH International Scientific Online Conference.
[20] Mathematical modeling of particle movement in laminar flow in a pipe. A Ibrokhimov, J.Orzimatov, M Usmonov, B Otakulov, S Mirzababayeva. BIO Web of Conferences 84, 02026.